Correlation-based wave-equation migration velocity analysis

Ali Almomin

ABSTRACT

Wave-equation migration velocity analysis (WEMVA) is a family of techniques that aim to improve the subsurface velocity model by minimizing the residual in the image space. Since the true image is unknown, measuring the residual in the image space is a challenge for WEMVA techniques. In this paper, I present a new method of measuring the image perturbation that is based on the cross-correlation of the observed image with a reference image in reflection angle gathers. I derive the gradient of this technique and show some synthetic examples that compare it to the optimum WEMVA gradient. I then modify the gradient in order to handle multiple events and show that it becomes immune to the problem of cycle skipping. I finally show a synthetic example of the modified gradient and compare it to the optimum gradient.

INTRODUCTION

Seismic velocity-analysis methods can be divided into two major groups. First, there are techniques that aim to minimize the misfit in the data domain, such as full waveform inversion (Tarantola, 1984; Luo and Schuster, 1991). Second, there are other techniques that aim to improve the quality in the image domain such as migration velocity analysis (MVA)(Symes and Carazzone, 1991; Biondi and Sava, 1999; Shen, 2004). These techniques try to measure the quality of the image and then invert the estimated image perturbation using a linearized wave-equation operator.

There are several advantages to minimizing the residual in the image space, such as increasing the signal-to-noise ratio and decreasing the complexity of the data (Tang et al., 2008). However, the biggest challenge in WEMVA techniques is that the true image is unknown. Therefore, each technique uses a certain attribute of the background image and tries to estimate the residual using that attribute. The stack-power-maximization technique maximizes the angle stack, and differential semblance optimization (DSO) minimizes the difference between neighboring traces in angle gathers. However, these assumptions can cause some problems, such as cycle-skipping in stack power maximization and edge effects in DSO.

In this paper, I present a new method of measuring the image residual that is based on the cross-correlation of the observed image with a reference image in reflection

angle gathers. The reference image can be any image with the desired kinematics, i.e. flat angle gathers. Therefore, it is possible to choose an angle stack as the reference image. However, angle stacks do not take into account the limited acquisition, which can result in anomalies in the gradient if the angle gathers are not muted properly. In order to take acquision into account, I create my reference image by computing Born-modeling data with the background slowness and a reference reflectivity. This reference reflectivity could come from the angle-stack image or from non-seismic data such as well-logs or geologic models. Therefore, modeling and migrating a dataset gives us more flexibility than just using the angle stack. The derivation of this method is based on traveltime inversion by Luo and Schuster (1991) but in the image domain instead of the data domain. After deriving the objective function and the gradient of this method, I provide some synthetic examples and compare the gradient to the optimum WEMVA gradient.

This technique is similar to differential residual migration (DRM) (Sava, 2004) in the sense that it uses the kinematics of a reference image. However, there are a few advantages in using correlation over DRM. First, the correlation method gives us more flexibility in choosing the reference image. Second, picking correlation lags could be automated more easily than picking DRM panels. Finally, the objective function of the correlation method could include the full correlation function as opposed to just maximum lags, which will eliminate picking and fully automate the inversion.

METHOD

The first step in evaluating a tomographic operator is to linearize the image $\mathbf{I}$ around the background slowness $\mathbf{s}_0$, as follows:

$$\mathbf{I} = \mathbf{I}_0 + \frac{\partial \mathbf{I}}{\partial \mathbf{s}}|_{s_0}(\mathbf{s} - \mathbf{s}_0) + ..., \tag{1}$$

where $\mathbf{I}_0$ is the background image and $\mathbf{s}$ is the slowness model. By neglecting the higher order terms in the image series, we can define the tomographic operator as follows:

$$\Delta \mathbf{I} = \frac{\partial \mathbf{I}}{\partial \mathbf{s}}|_{s_0}\Delta \mathbf{s} = \mathbf{T}\Delta \mathbf{s}, \tag{2}$$

where $\mathbf{T}$ is the tomographic operator. Now, we use the conventional imaging condition as follows:

$$I(\mathbf{x}, \mathbf{h}) = \sum_{\omega, \mathbf{x}_s, \mathbf{x}_r} G^*(\mathbf{x} - \mathbf{h}, \mathbf{x}_s, \omega) G^*(\mathbf{x} + \mathbf{h}, \mathbf{x}_r, \omega) d(\mathbf{x}_r, \mathbf{x}_s, \omega), \tag{3}$$

where I is the image, G is the Green's function, d is the surface data, ω is frequency, $\mathbf{x}_s$ and $\mathbf{x}_s$ are the source and receiver coordinates, and $\mathbf{h}$ is the subsurface offset. To evaluate the tomographic operator $\mathbf{T}$, I take the derivative of the imaging condition

as follows:

$$\begin{aligned}\Delta I(\mathbf{x},\mathbf{h}) &= \sum_{\mathbf{y}} \frac{\partial I(\mathbf{x},\mathbf{h})}{\partial s(\mathbf{y})}\Delta s(\mathbf{y}) \\ &= \sum_{\omega,\mathbf{x}_s,\mathbf{x}_r,\mathbf{y}} \left\{-2\omega^2 s_0(\mathbf{y}) G_0^*(\mathbf{y},\mathbf{x}_s,\omega) G_0^*(\mathbf{x}-\mathbf{h},\mathbf{y},\omega)\right\} G_0^*(\mathbf{x}+\mathbf{h},\mathbf{x}_r,\omega) d(\mathbf{x}_r,\mathbf{x}_s,\omega)\Delta s(\mathbf{y}) \\ &+ \sum_{\omega,\mathbf{x}_s,\mathbf{x}_r,\mathbf{y}} \left\{-2\omega^2 s_0(\mathbf{y}) G_0^*(\mathbf{x}-\mathbf{h},\mathbf{x}_s,\omega) G_0^*(\mathbf{x}+\mathbf{h},\mathbf{y},\omega)\right\} G_0^*(\mathbf{y},\mathbf{x}_r,\omega) d(\mathbf{x}_r,\mathbf{x}_s,\omega)\Delta s(\mathbf{y}),\end{aligned} \tag{4}$$

where y is the slowness coordinate. The full derivation of the tomographic operator is presented in Almomin and Tang (2010).

After defining the tomographic operator, I use a cross-correlation function to estimate image perturbations:

$$f(\zeta,\gamma;\mathbf{x}) = \sum_z I_{\text{obs}}(z,\gamma;\mathbf{x}) I_{\text{cal}}(z+\zeta,\gamma;\mathbf{x}), \tag{5}$$

where ζ is the lag, γ is the reflection angle, $\mathbf{x}$ is the surface coordinates, z is depth, I_{obs} is the angle-domain image using the observed data, and I_{cal} is the angle-domain image using the calculated data, which is modeled with the background slowness. I_{cal} is always going to be flat, since I create Born-modeled data using a reference model as the reflectivity and the background slowness and then migrate that data using the same background slowness. Next, I define ξ to be the lag that maximizes the correlation function. Therefore, the derivative of the correlation function vanishes at that lag, as follows:

$$\mathbf{g} = \frac{\partial \mathbf{f}}{\partial \zeta}|_{\xi} = \sum_z \frac{\partial}{\partial z} I_{\text{obs}}(z,\gamma;\mathbf{x}) I_{\text{cal}}(z+\xi,\gamma;\mathbf{x}) = 0. \tag{6}$$

We can now use ξ as our measure of the residual to minimize, casted as the following objective function:

$$J(\mathbf{s}) = \frac{1}{2}\|\xi(\gamma,\mathbf{x})\|^2. \tag{7}$$

Then, we take the derivative of the objective function with respect to slowness as follows:

$$\nabla J = \left(\frac{\partial \xi}{\partial \mathbf{s}}\right)^* \xi, \tag{8}$$

where * indicates an adjoint. By using the chain rule of differentiation, I relate the derivative of the maximum lag ξ with respect to $\mathbf{s}$ to the derivative of the correlation function with respect to $\mathbf{s}$ as follows:

$$\left(\frac{\partial \xi}{\partial \mathbf{s}}\right)^* = \left(\frac{\partial \mathbf{g}}{\partial \mathbf{s}}\frac{\partial \xi}{\partial \mathbf{g}}\right)^*. \tag{9}$$

The second partial derivative in equation (9) is just a scalar that balances the energy between surface locations. The first partial derivative with respect to slowness can be calculated using equation (6) as follows:

$$\left(\frac{\partial \mathbf{g}}{\partial \mathbf{s}}\right)^* = \sum_z \left(\frac{\partial I_{\rm obs}(z,\gamma;\mathbf{x})}{\partial \mathbf{s}}\right)^* \frac{\partial}{\partial z} I_{\rm cal}(z+\xi,\gamma;\mathbf{x}) + \sum_z \left(\frac{\partial I_{\rm cal}(z+\xi,\gamma;\mathbf{x})}{\partial \mathbf{s}}\right)^* \frac{\partial}{\partial z} I_{\rm obs}(z,\gamma;\mathbf{x}). \quad (10)$$

The first tomographic operator in equation (10) can be computed as I described in equation (4). However, the second tomographic operator depends on how $I_{\rm cal}$ is computed. If a fixed-reflectivity model is used, such as well data, and only the background slowness is updated, then this derivative will be very small and could be ignored, since changing the slowness updates does not change the reflectivity estimate. On the other hand, if we allow the modeling reflectivity to change location, i.e. we update the reflectivity model as we iterate, then this operator could have a significant component. However, evaluating this operator is much more expensive than the first tomographic operator, since it is a cascade of three operators. Therefore, I will assume that the first tomographic operator is sufficient and ignore the second term.

SYNTHETIC EXAMPLES

The background model has a constant velocity of 2500 m/s. The model is 4000 m wide and 2800 m deep. The spatial sampling is 20 m, and the temporal sampling is 3 ms. A Ricker wavelet with a fundamental frequency of 15 Hz is used to model the data. The receiver spacing is 20 m, and the shot spacing is 80 m. The reflector is at a depth of 2200 m. Born modeling was used in both the observed and the calculated data. There are three anomalies that I will estimate: first, a negative Gaussian anomaly at a depth of 1300 m with a maximum velocity of 800 m/s, second, a constant velocity decrease of 250 m/s, and third, a constant velocity increase of 250 m/s. First, I will compute the optimum WEMVA gradient by applying the forward and adjoint of these slowness perturbations. The results are shown in figures 1(a), 1(c) and 1(e). Then, I compute the angle-domain common-image gathers using the background velocity of the data with the three anomalies, which are shown in figures 1(b), 1(d) and 1(f).

Next I show the results of applying the first term of the tomographic operator in equation (10). First, I use the true reflector depth to create the reference image and use it in our method to generate the gradients for the three anomalies, as shown in figures 2(a), 2(c) and 2(e). Finally, I use the apparent reflector depth, i.e. the depth extracted from the zero-subsurface-offset image, to create the reference image and generate the gradients shown in figures 2(b), 2(d) and 2(f). The correlation lags were picked automatically by choosing the maximum value of the cross-correlation function.

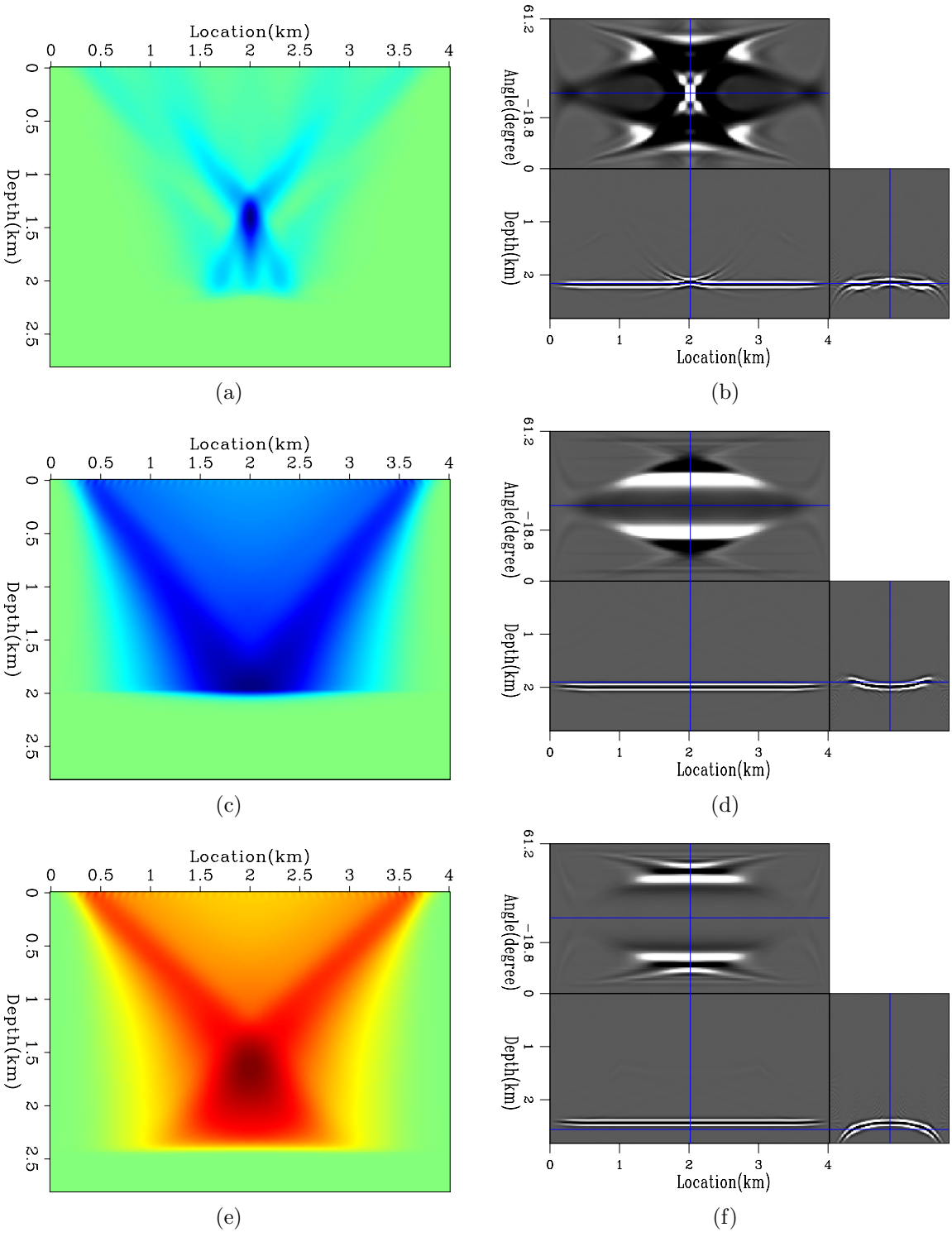

Figure 1: The left column shows the optimum WEMVA gradient of (a) a negative Gaussian anomaly, (c) a negative bulk shift and (e) a positive bulk shift. The right column shows the corresponding ADCIGs. [**CR**]

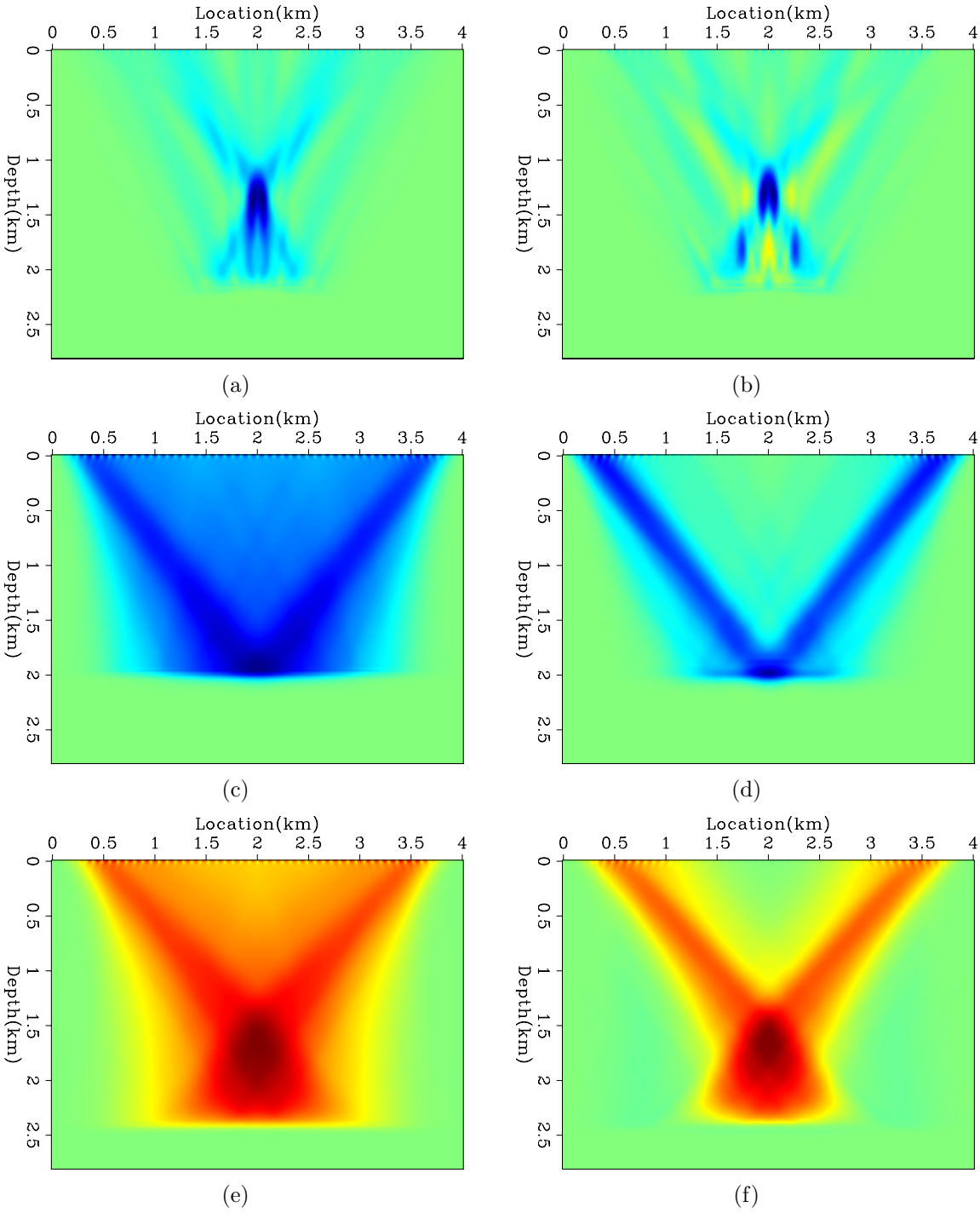

Figure 2: The left column shows the correlation-based WEMVA gradients using the true depth for the reference image. The right column shows the correlation-based WEMVA gradients using the apparent depth for the reference image. [**CR**]

Modified correlation-based WEMVA

There were two disadvantages to the original correlation-based WEMVA gradient. First, it assumes a single correlation lag per trace. Second, it is sensitive to the actual values of the picked correlation lags. If these lags are not correct, the gradient might have a cycle-skipping problem. In order to overcome these disadvantages, I approximate the shifted flat image by the observed image to get the following modified gradient:

$$\nabla J = \sum_z \left(\frac{\partial I_{\text{obs}}(z,\gamma;\mathbf{x})}{\partial \mathbf{s}} \right)^* \frac{\partial}{\partial z} I_{\text{obs}}(z,\gamma;\mathbf{x}) \frac{\xi}{E} \tag{11}$$

This modified gradient is immune to cycle-skipping since the residual and operator match by design. In addition, it is not as sensitive to the values of the picked lags. Finally, multiple picked lags could be used in this formulation.

Figures 3(a) and 3(b) show the true and background velocities of a salt model. ADCIGs using these two velocities on the observed data are shown in figures 4(a) and 4(b). Next, I used a sliding Gaussian window to compute and pick local cross-correlation panels between the observed image and the stacked image. Then, I picked the maximum correlation lag at each depth level. The picked lags are shown in figure 5.

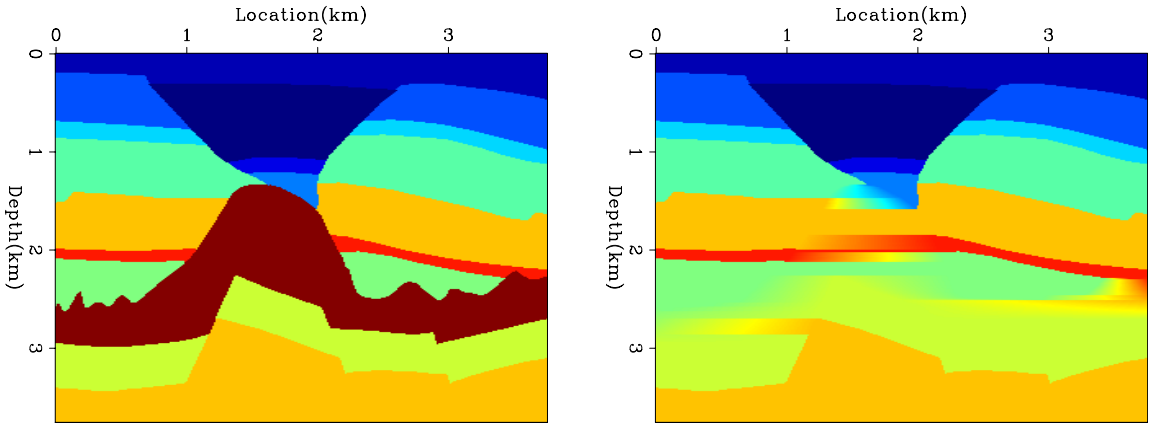

(a) (b)

Figure 3: The true velocity salt model (a) and the background velocity model (b). [**ER**]

As in the previous example, I computed the optimum gradient using the true velocity anomaly and the modified correlation-based WEMVA gradient using the picked correlation lags. These two gradients are shown in figure 6(a) and 6(b). Although we used the apparent depth of the stacked image, the modified gradient shows very good results that are very similar to the optimum gradient. In this case, the velocity information in large reflection angles was more dominant than those in zero reflection angle.

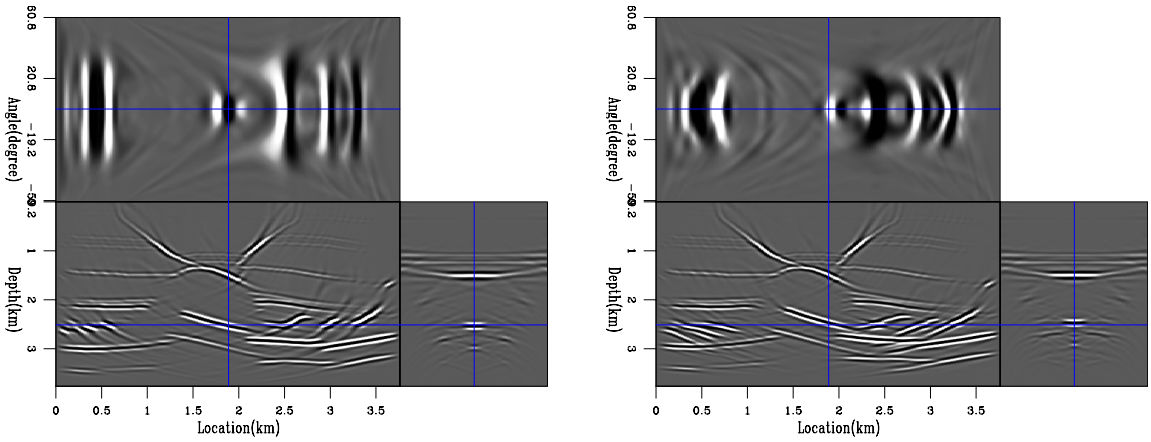

Figure 4: ADCIGs using the true velocity salt model (a) and using the background salt model (b). [**CR**]

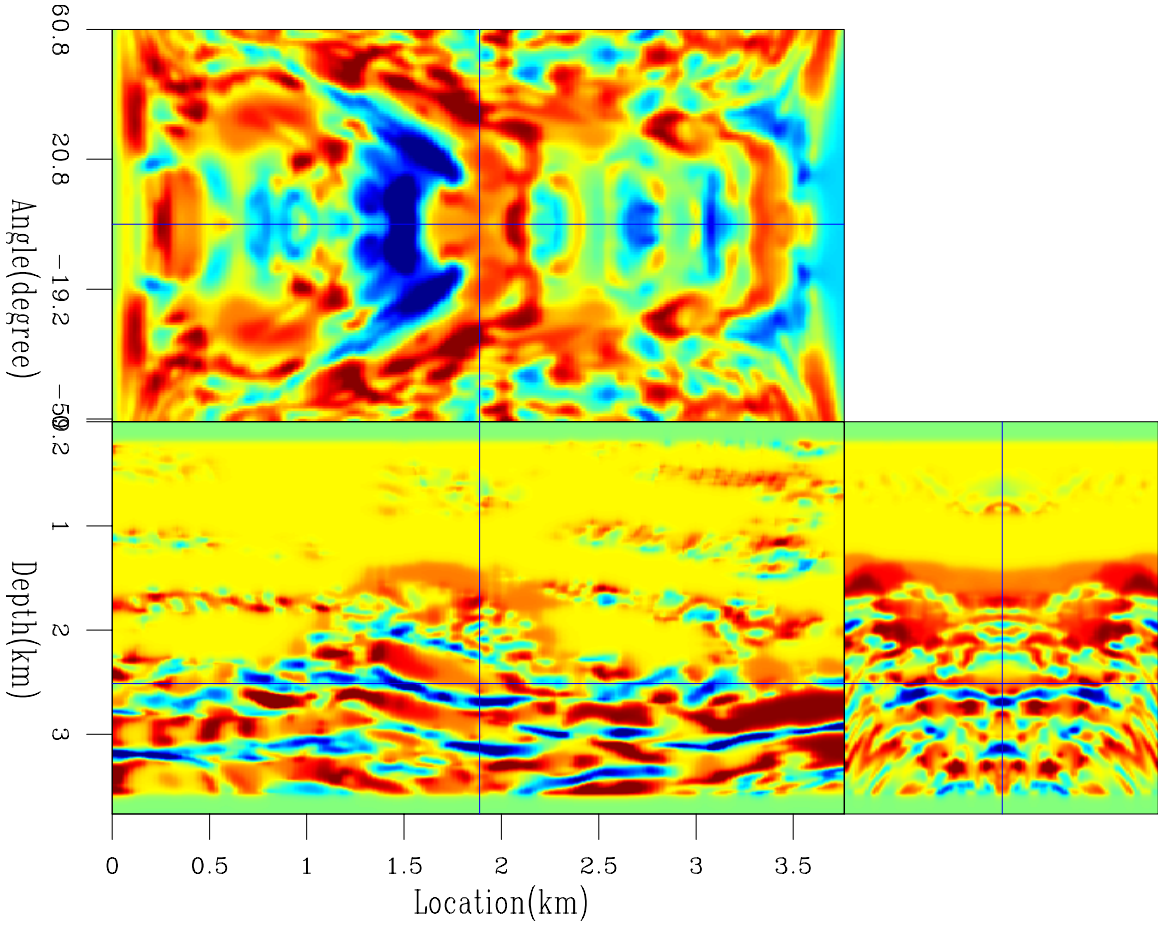

Figure 5: Lag estimation of the maximum local correlation. [**CR**]

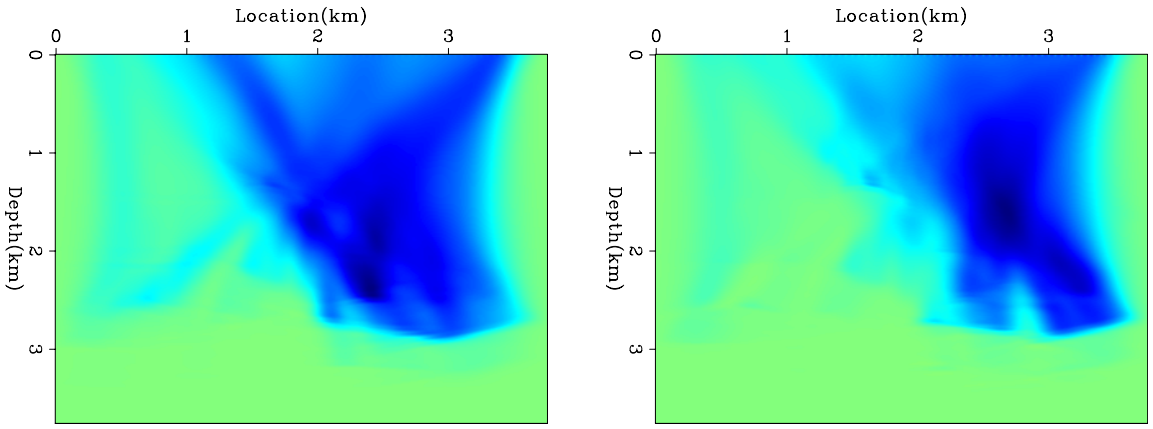

(a) (b)

Figure 6: The optimum WEMVA gradient of the salt model (a) and the modified correlation-based WEMVA gradient of the salt model (b). [**CR**]

DISCUSSION AND CONCLUSIONS

By examining the results, we see that, when provided with the true depth, the correlation-based WEMVA produces excellent results with no cycle-skipping or edge effects. When the apparent depth was provided, the results start to have some errors. However, these errors are to be expected due to the velocity-depth ambiguity. Therefore, the gradients will flatten the gathers but not necessarily resolve the correct depth (Zhang and Biondi, 2011). However, the results are still satisfactory, since the gradient is pointing toward the right direction.

Using the modified gradient has several advantages, such as handling multiple events. However, I need to further test the approximations made in the modified gradient. Leeuwen (2010) showed that it is possible to further improve the objective function by multiplying with the proper weights and minimizing the correlation function instead of the lags, which will eliminate any picking. Finally, using correlation functions over extended images (Yang and Sava, 2009) could help provide better results.

REFERENCES

Almomin, A. and Y. Tang, 2010, Migration velocity analysis based on linearization of the two-way wave equation: SEP-Report, **142**, 13–24.

Biondi, B. and P. Sava, 1999, Wave-equation migration velocity analysis: SEG Technical Program Expanded Abstracts, **18**, 1723–1726.

Leeuwen, T. V., 2010, Correlation-based seismic velocity inversion: PhD thesis, Delft University of Technology.

Luo, Y. and G. T. Schuster, 1991, Wave-equation traveltime inversion: Geophysics, **56**, 645–653.

Sava, P., 2004, Migration and velocity analysis by wavefield extrapolation: PhD thesis, Stanford University.

Shen, P., 2004, Wave equation migration velocity analysis by differential semblance optimization: PhD thesis, Rice University.

Symes, W. W. and J. J. Carazzone, 1991, Velocity inversion by differential semblance optimization: Geophysics, **56**, 654–663.

Tang, Y., C. Guerra, and B. Biondi, 2008, Image-space wave-equation tomography in the generalized source domain: SEP-Report, **136**, 1–22.

Tarantola, A., 1984, Inversion of seismic reflection data in the acoustic approximation: Geophysics, **49**, 1259–1266.

Yang, T. and P. Sava, 2009, Wave-equation migration velocity analysis using extended images: SEG Expanded Abstracts, **28**, 3715–3719.

Zhang, Y. and B. Biondi, 2011, Moveout-based wave-equation migration velocity analysis: SEP-Report, **143**, 43–58.

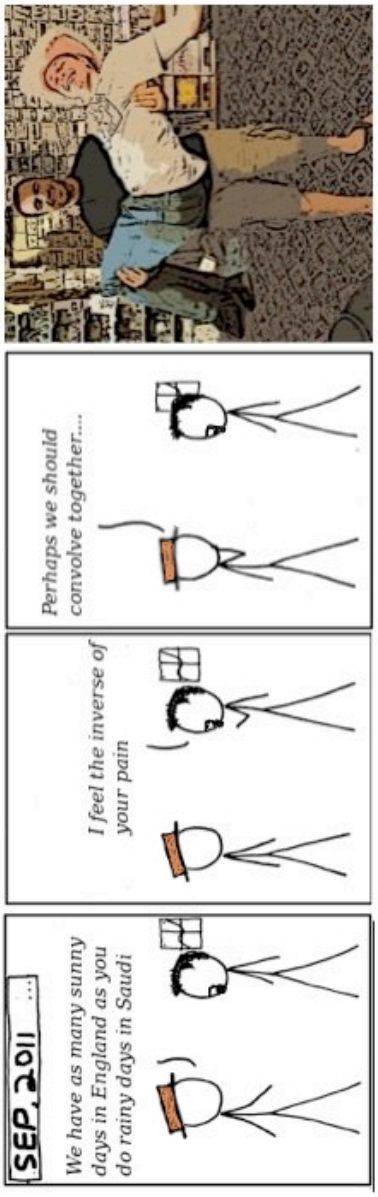
SEP, 2011 ...
We have as many sunny days in England as you do rainy days in Saudi
I feel the inverse of your pain
Perhaps we should convolve together....